Journal of Renewable Materials

Tech Science Press

https://doi.org/10.32604/jrm.2026.02025-0229

ARTICLE

Towards the Development of Innovative Bio-Based Flame-Retardant Systems Derived from Phosphorylated Condensed Tannins

K. Tilouche-Guerdelli, C. Lacoste*, D. Perrin and A. Bergeret*

Polymers Composites and Hybrids (PCH), IMT Mines Ales, Ales, France

*Corresponding Authors: C. Lacoste. Email: clement.lacoste@mines-ales.fr; A. Bergeret. Email: anne.bergeret@mines-ales.fr

Received: 20 January 2026; Accepted: 17 April 2026; Published: 29 June 2026

ABSTRACT: In this study, tannins were investigated as sustainable flame retardants. The thermal and structural properties of tannic acid, chestnut, oak, and quebracho extracts were first characterized by Fourier Transform Infrared Spectroscopy (FTIR), Thermogravimetric Analysis (TGA), and Pyrolysis Combustion Flow Calorimetry (PCFC). Quebracho exhibited the most promising thermal performance, showing the lowest heat release and the highest char yield (≈38 wt.%). To further improve their efficiency, quebracho tannins were phosphorylated using phytic acid (QPHYA) or phosphoric acid (QPHOA). Phosphorus contents reached 13% and 15%, respectively, as confirmed by ICP and SEM–EDX analyses, while FTIR and NMR evidence the formation of new P–O bonds. Phosphorylation enhanced thermal stability, increasing char yield up to 52%. Flax rovings (TR, 500 tex) were treated with tannin formulations using an impregnation line. The treated rovings exhibited higher impregnation efficiency ($\Delta\% \approx 18$) and phosphorus uptake (up to 3.7 wt.%). SEM–EDX analysis confirmed deeper penetration of the tannin-based agents within the rovings, while FTIR spectra revealed the appearance of phosphorus-related P–O and P=O absorption bands, suggesting phosphorus incorporation and treatment-induced interactions. TGA results demonstrated that phosphorylated rovings produced significantly higher char residues (33%–38%) compared to untreated flax (16%) and non-phosphorylated counterparts (≈21%). Overall, these findings highlight phosphorylated quebracho tannins as efficient and eco-friendly flame retardants, where the impregnation efficiency and phosphorus retention are strongly influenced by the fiber architecture.

KEYWORDS: Tannins; phytic acid; phosphorylation; flax roving functionalization; thermal stability and char yield

1 Introduction

In France, more than 234,702 fires were reported in 2025, causing significant human and economic losses [1]. Flame retardants (FRs) are therefore essential in applications such as textiles, polymers, and composites used in construction, transportation, and electronics. Conventional FRs, including halogenated, mineral, nitrogen-, or phosphorus-based systems [2], are effective but raise environmental and processing concerns, which have accelerated the search for bio-based, sustainable alternatives [3].

The improvement of fire resistance in materials is a major challenge. FRs can act physically or chemically in the condensed or gaseous phases, depending on their nature [4]. Physically, they may (i) cool materials through endothermic decomposition, (ii) release inert gases to dilute fuels, or (iii) form protective layers that limit heat transfer and pyrolysis gases release. Chemically, FRs delay combustion by releasing radicals that neutralize highly reactive species, reducing heat release and fuel production. In the condensed phase, they may also form carbonized layers acting as protective barriers [5].

Halogenated FRs [6–9] (brominated, fluorinated, chlorinated) are among the most effective, as they provide high efficiency at relatively low loadings (typically 15–20 wt.%), but their use is increasingly restricted because of toxic gas and smoke release during combustion. In contrast, mineral fillers such as aluminium and magnesium hydroxides [9] are halogen-free and environmentally benign but require much higher loadings (>50 wt.%), which significantly compromise mechanical properties and processing ability. Nitrogen-based FRs (e.g., melamine and its salts) act through endothermic decomposition, releasing inert gases and forming protective barriers, while phosphorus-based FRs [9] (organic phosphates, ammonium polyphosphates, red phosphorus) are considered promising since they act in both the gaseous and condensed phases through radical trapping and char formation [10]. To address resource depletion, bio-based FRs have been explored [11,12]. Polysaccharides such as cellulose [13–16] hemicellulose [17,18] chitosan [19], starch [20,21] cyclodextrin, and isosorbide, as well as phenolic compounds like lignin [16,22] and cardanol [23] have been applied to thermoplastics, thermosets, and textiles. These can be used directly or after functionalization with phosphorus, boron, or nitrogen [9,24–26]. Recent reviews have highlighted the growing interest in eco-friendly, bio-based flame retardants for natural fiber-reinforced polymer composites, emphasizing phosphorus-containing systems and char-forming biopolymers as promising alternatives to conventional flame retardants [4,15].

Among these, tannins are of particular interest due to their (i) abundance in biomass and non-toxicity, (ii) strong natural char-forming ability, and (iii) multiple hydroxyl groups enabling chemical functionalization [4]. Tannins are polyphenolic biopolymers predominantly located in the wood and bark of plants, where they play a crucial role in providing antimicrobial defense and thermal protection [27]. They are broadly classified into two principal groups: hydrolysable tannins, comprising gallotannins and ellagitannins, and condensed tannins [26,28] which are polymers formed from flavonoid subunits [29].

Hydrolysable tannins such as tannic acid have shown improved fire performance in wood, cardboard [30], textiles [27,30,31], and polymers [29,32]. Xia et al. [33] reported increased LOI values for cotton nonwovens treated with tannic acid, attributed to its barrier-forming ability. Korey et al. [29] demonstrated that tannic acid enhanced epoxy thermal stability and flame resistance. Condensed tannins are economically important, representing >90% of global tannin production [34]. They are composed of flavonoid oligomers with inter flavanol linkages, generally at C4–C6 or C4–C8, depending on the ring hydroxylation patterns [35]. Previous studies have shown that condensed tannins yield 30%–50% char upon decomposition [35–37].

To improve efficiency, tannins and other polyphenols have been functionalized with phosphorus [5], boron or nitrogen. Among these strategies, phosphorylation has received particular attention, as it enables the introduction of phosphate groups capable of promoting char formation and radical trapping during combustion [37]. The phosphorylation of condensed tannins was first demonstrated by Basso et al. [5], who reported the reaction of flavonoid tannins with triethyl phosphate and evidenced oligomerization and crosslinking through spectroscopic analyses. This pioneering work established the chemical feasibility of introducing phosphate functionalities into condensed tannin structures. Subsequent studies have mainly focused on hydrolysable tannins or on bulk polymer formulations. For example, phosphorus derivatives of hydrolysable tannins have improved the flame resistance of PLA [38]. Phytic acid, a naturally abundant phosphorus source (28 wt.% P), has also been investigated as an eco-friendly phosphorylating agent [39], applied to polymers [40,41] and textiles [38,42,43]. Marques et al. [44] demonstrated enhanced fire resistance when tannins and phytic acid were combined within intumescent paints. Similar synergistic flame-retardant effects between tannic acid and phytic acid have also been reported in textile systems [43,44]. Recent studies have demonstrated that the incorporation of bio-based flame-retardant systems in natural fiber-reinforced composites can significantly improve fire performance, including increased LOI values and char residue, while maintaining sustainability considerations [45].

However, although the chemical phosphorylation of condensed tannins has been demonstrated [5], their direct use as flame retardants, particularly in fiber-reinforced composite systems, remains scarcely investigated. In particular, the combination of controlled phosphorylation chemistry with direct application onto reinforcing fibers has not yet been systematically explored.

In this study, condensed quebracho tannins were investigated as flame retardants through a controlled phosphorylation and fiber impregnation strategy using phytic acid and phosphoric acid as phosphorus sources. Unlike previous works that mainly addressed hydrolysable tannins or bulk polymer formulations, this study combines phosphorus incorporation at the molecular scale with direct impregnation of flax rovings, enabling evaluation of phosphorus-modified condensed tannins at the fiber level.

This dual-scale approach provides new insights into structure–property–fire performance relationships in bio-based flame-retardant systems and offers a scalable route toward sustainable fire-safe composites. The efficiency of the strategy was assessed using complementary characterization techniques (FTIR, TGA, PCFC, NMR, ICP, and SEM–EDX) to establish correlations between phosphorus incorporation, thermal behavior, and flame-retardant performance.

2 Materials and Methods

2.1 Materials

This study investigated four commercially available powdered tannins, comprising three hydrolysable variants: (i) tannic acid (Ta), (ii) chestnut tannin (C), and (iii) oak tannin (K). Quebracho tannin (Q) was selected as a representative condensed tannin. Oak, chestnut, and quebracho extracts were supplied by Silva Chimica (Italy), while tannic acid was purchased from Fluka (Darmstadt, Germany). Tannic acid, a hydrolysable gallotannin, consists of glucose units esterified with phenolic groups, interconnected through ester or ether linkages (Fig. 1a). Chestnut and oak tannins (Fig. 1b), derived from *Castanea sativa* and Quercus species, are mainly composed of gallic (Fig. 1c) and ellagic acids (Fig. 1d), with chestnut tannins also containing catechic acids [46]. Condensed tannins were extracted from quebracho wood (*Schinopsis* sp.) and are mainly composed of flavonoid units rich in fisetinidin relative to robinetinidin (Fig. 1e). These tannins exhibit a predominantly linear structure [47]. Phytic acid (50 wt.% aqueous solution) was supplied by Analytic Lab (France) (Fig. 1f), while phosphoric acid (85 wt.% aqueous solution, Fig. 1g) and urea (99.5% purity) were obtained from Acros Organics (Belgium).

2.2 Methodology for the Phosphorylation of Condensed Quebracho Tannins

Phosphorylated tannins were synthesized from raw quebracho condensed tannins using either phosphoric acid (QPHOA) or phytic acid (QPHYA), following a three-step protocol. In the first step, phytic or phosphoric acid was introduced into a 200 mL flask heated at 80°C in an oil bath, after which urea (25 g) was gradually added under continuous stirring for 30 min. This reaction yielded ammonium phytate salts (with phytic acid) or ammonium polyphosphate salts (with phosphoric acid), which promote tannin phosphorylation by forming stable complexes that enhance tannin solubility in aqueous media. As previously reported for phosphorylated lignin [48], urea also improves thermal stability and contributes to the intumescent effect by releasing nitrogen gases upon decomposition. In the second step, raw quebracho tannins (40 g) were progressively added to the solution under vigorous stirring at 80°C for 1 h, leading to the formation of phosphorylated tannins (QPHYA or QPHOA). In the third step, the functionalized tannins were recovered by Büchner filtration, dried overnight at 80°C, and subsequently heat-cured at 150°C for 2 h to activate crosslinking. Residual acids were removed through repeated centrifugation (at 10,000 rpm) until a neutral pH was reached. Finally, the phosphorylated tannins were collected, dried at 60°C for 24 h,

and ground using a Retsch ZM 200 grinder (1 mm screen) to obtain functionalized tannin powders with a maximum particle size of 1 mm (Fig. 2).

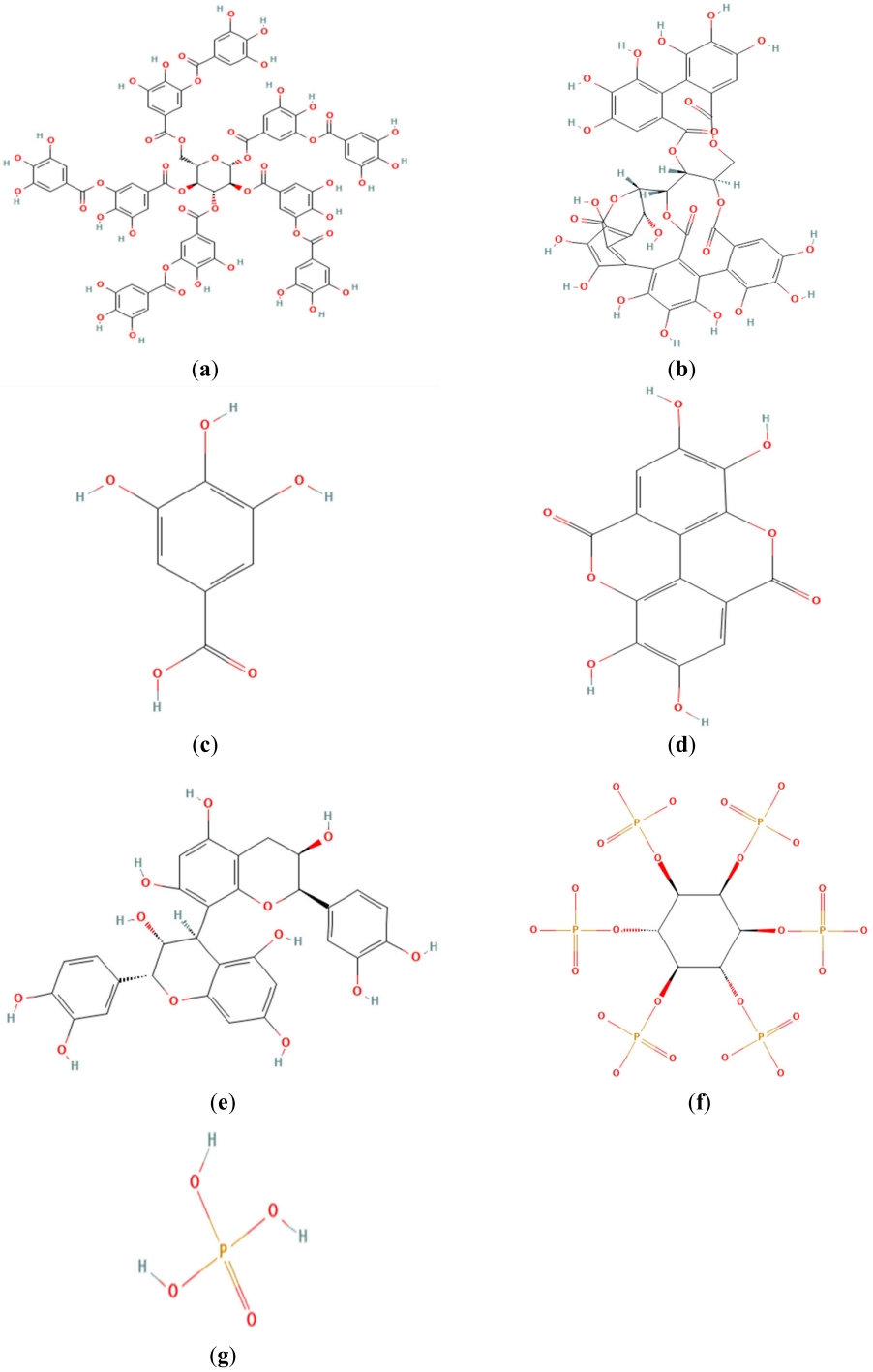

Figure 1: Structure of (**a**) tannic acid, (**b**) chestnut and oak ellagitannins, (**c**) gallic acid, (**d**) ellagic acid, (**e**) quebracho tannins, (**f**) phytic acid and (**g**) phosphoric acid.

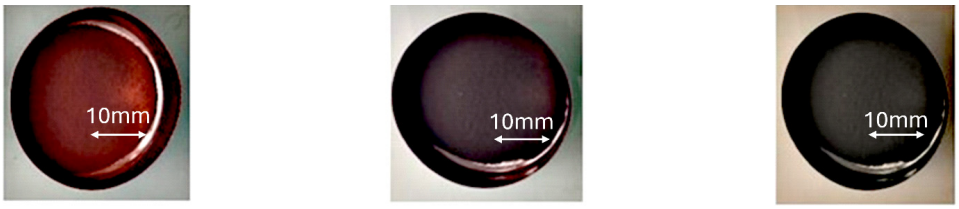

(a) (b) (c)

Figure 2: Raw quebracho tannins (**a**) Q, and phosphorylated tannins prepared with (**b**) phytic acid (QPHYA) and (**c**) phosphoric acid (QPHOA).

2.3 Thermogravimetric Analysis (TGA)

Thermogravimetric analysis (TGA) was performed using a SETSYS Evolution instrument (Setaram, France) to monitor mass variation of the samples under a controlled temperature program. Sample weights ranged between 10 and 15 mg. Heating was conducted from 30 to 900°C at a rate of 10°C/min under a nitrogen atmosphere. The onset decomposition temperature (T_{onset}) was defined at 5% mass loss, while the maximum degradation rate temperature was determined from the derivative thermogravimetric (DTG) curve. Residual mass was measured at 900°C. All measurements were carried out in triplicate to ensure reproducibility.

2.4 Pyrolysis Combustion Flow Calorimetry (PCFC)

Microscale fire behavior was assessed using a pyrolysis combustion flow calorimeter (PCFC, Fire Testing Technology Ltd., U.K.), following ASTM D7309. Approximately 5 mg of sample was pyrolyzed under nitrogen from 90°C to 750°C at a heating rate of 1°C/s. The resulting degradation gases were transferred into a combustion chamber by the nitrogen flow, then mixed with oxygen in a high-temperature furnace to ensure complete combustion. The heat release rate (HRR) was recorded as a function of temperature, while the total heat release (THR) was obtained from the area under the HRR curve. The peak heat release rate (pHRR) was defined as the maximum value of the HRR profile. All measurements were carried out in triplicate to ensure reproducibility.

2.5 Preparation of Synthesized Phosphorylated Tannin Solutions for the Functionalization of Flax Fibers

Quebracho tannin powder (Q) or phosphorylated tannins (QPHYA and QPHOA) were diluted in water at a concentration of 5 wt% and stirred for 40 min. The initial pH of the solution was around 5. Upon addition of a 1 wt% NaOH solution and continued stirring to ensure complete homogenization, the final pH reached approximately 11. The addition of NaOH served to regulate the pH, thereby creating optimal treatment conditions while preventing flax fiber degradation. Furthermore, the pH increase promoted the activation of tannins during the condensation reaction with flax fibers, enhancing the efficiency of the treatment and potentially improving tannin adhesion to the fibers, which in turn may enhance the properties of the resulting materials. Flax rovings (TR) were impregnated using a continuous impregnation line (previously detailed in [49]). Briefly, the setup consists of successive unwinding, immersion, squeezing, and drying stages ensuring uniform tannin uptake. The nomenclature used throughout this study is as follows.

QPHYA: Phosphorylated quebracho tannins using phytic acid
QPHOA: Phosphorylated quebracho tannins (sing phosphoric acid)
N: NaOH solution
TRQ5N1: Flax rovings treated with 5 wt.% quebracho tannin and 1 wt.% NaOH.
TRQPHYA5N1: Flax rovings treated with 5 wt.% phosphorylated quebracho tannins (using phytic acid) and 1 wt.% NaOH.
TRQPHO5N1: Flax rovings treated with 5 wt.% phosphorylated quebracho tannins (using phosphoric acid) and 1 wt.% NaOH.

3 Results and Discussion

3.1 Characterization of the Hydrolysable and Condensed Tannins

The chemical structures of the investigated tannins, including quebracho tannin, are well established in the literature and are briefly recalled here to facilitate interpretation of the FTIR spectra and subsequent discussion of their thermal behavior and reactivity. ATR-FTIR spectra of the four tannins are shown in Fig. 3. The region between 2000 and 400 cm^{-1}, considered the most informative, is detailed in Fig. 2b. All spectra display a broad OH stretching band (3600–3400 cm^{-1}) and weak CH2 peaks at 3000–2800 cm^{-1}, partially overlapped by the OH band. Hydrolysable tannins (Ta, C, K) show similar spectral features, distinct from condensed tannins (Q), reflecting their different chemical structures. Four bands common to all tannins were identified at 1606–1589, 1529–1515, 1446–1440, and 1043–1030 cm^{-1}, corresponding to aromatic C=C stretching, skeletal vibrations, and C–O stretching, consistent with the literature. Hydrolysable tannins also presented additional characteristic signals: bands at 1180–1189 cm^{-1} (C–O stretching) and ~750 cm^{-1} (sugar ring vibrations). In tannic acid, bands at 1695 and 1315 cm^{-1} indicate phenolic esters and lactone C–O stretching, while oak and chestnut showed similar bands at 1720 and 1309 cm^{-1}. A shoulder near 879 cm^{-1} suggests the presence of gallotannin. The slight shifts in C=O and C–O–C positions between Ta, C, and K reflect differences in polymeric complexity, with oak and chestnut being structurally more heterogeneous than tannic acid. In contrast, quebracho exhibited the typical features of condensed tannins: bands at 1355 cm^{-1} (C–O phenol/O–H deformation), 1245 cm^{-1} (C–O pyran ring, flavonoids), 1203 cm^{-1} (aromatic C–OH), 1030 cm^{-1} (C–O–C cyclic ethers), and 763 cm^{-1} (aromatic C–H). Altogether, FTIR analysis allowed the identification of characteristic functional groups of both hydrolysable and condensed tannins, confirming the presence of reactive sites available for subsequent phosphorylation and functionalization.

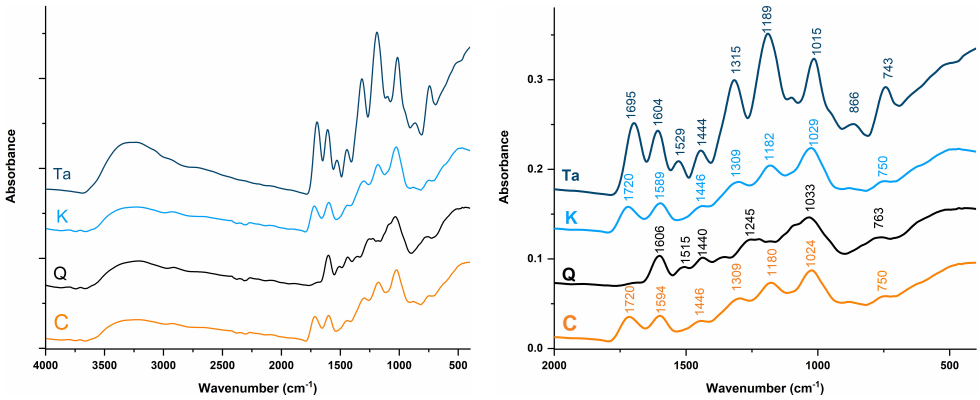

Figure 3: FTIR spectra of tannins including tannic acid (Ta), oak tannin (K), quebracho tannin (Q), and chestnut tannin (C), (**a**) Full spectral range (4000–400 cm^{-1}), (**b**) Expanded view of the fingerprint region (2000–400 cm^{-1}).

Thermogravimetric analysis (TGA) under nitrogen (Fig. 4) was used to evaluate the thermal degradation and char formation of tannic acid, quebracho, chestnut, and oak tannins. Results showed that the chemical structure strongly influences the degradation pathways: condensed tannins decompose in three main stages, while hydrolysable tannins exhibit five distinct steps. The additional transitions observed for hydrolysable tannins are attributed to the breakdown of ester-linked sugars and polyphenolic units, whereas condensed tannins follow a more simplified degradation route. These differences highlight the structural dependence of char formation, which is a key parameter in flame-retardant efficiency.

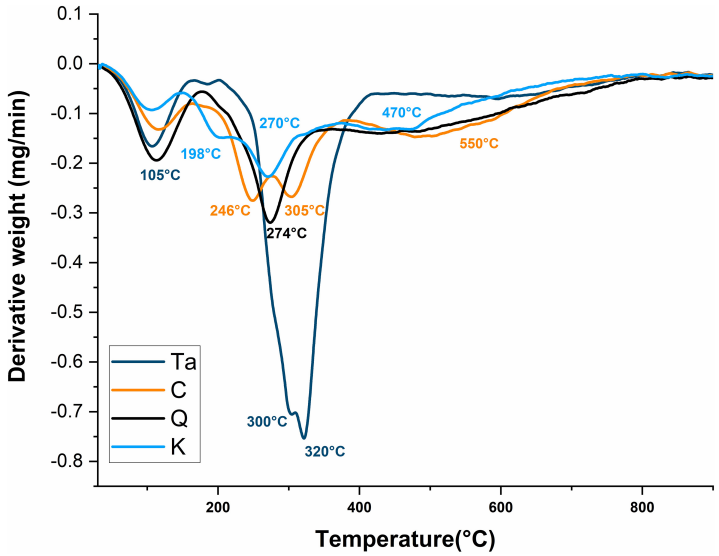

Figure 4: Thermogravimetric analysis (TGA) curves of different tannins (Ta: tannic acid; K: oak tannin; Q: quebracho tannin; C: chestnut tannin) recorded at a heating rate of 10°C·min^{-1} under nitrogen atmosphere.

For tannic acid, the first weight loss at ~105°C corresponds to the release of volatile fractions such as aldehydes, ketones, and carboxylic acids. At ~300°C, degradation starts with decarboxylation of the outer gallic acid units and cleavage of ester bonds. A further stage at ~320°C involves decarboxylation of inner gallic acids, releasing aromatic compounds and CO_2, together with ester bond cleavage between gallic acids and glucose. This step is also marked by cross-linking between gallic acid units, promoting char formation. Tannic acid displayed a char yield of ~20 wt.% at 600°C, decreasing to ~8 wt.% at 900°C (Fig. 4). Consistent with these results, Xia et al. [33] reported that tannic acid undergoes multi-step thermal degradation under an inert atmosphere, producing an intumescent char that serves as a thermally stable barrier layer at elevated temperatures. For chestnut and oak tannins, the first degradation occurs at 100°C–120°C due to moisture removal. The main decomposition stage proceeds in two steps: 190°C and 270°C for oak, and at 246°C and 305°C for chestnut. This corresponds to saccharide decomposition, in agreement with Karaseva et al. [50] who reported similar behavior between 200°C–350°C. Further steps at ~470°C (oak) and ~550°C (chestnut) are associated with ellagic acid and ellagitannin decomposition. Char yields at 600°C are ~36% and 40% for oak and chestnut, decreasing to 26% and 29% at 900°C, respectively (Fig. 5). Their high char yields arise from their complex composition, particularly rich in ellagitannins that promote carbonization, with saccharides further enhancing char formation [51]. TGA thus confirms the similar thermal decomposition patterns of these two hydrolysable tannins. Quebracho tannin shows a three-step degradation. The first step, at ~105°C, corresponds to moisture evaporation due to its hygroscopicity. The second, at ~274°C, is attributed to decarboxylation. Beyond ~500°C, carbonization of polyflavonoids occurs, releasing small molecules [30], including catechin and catechol during pyrolysis of condensed tannins [37]. According to Konai et al. [52], the

final degradation step involves decomposition of flavonoid structures, particularly the A and B rings. Given its high proportion of resorcinol structures, quebracho tannin consists mainly of catechin fragments with two dihydroxybenzene rings. Thermal decomposition of this aromatic network favors reticulation reactions, leading to intense char formation. The char yields reached 49% at 600°C and 38% at 900°C (Fig. 5). The superior thermal performance of quebracho tannin compared to hydrolysable tannins can be directly related to its chemical structure. Quebracho tannin is a condensed tannin composed mainly of polyflavonoid units linked through stable C–C bonds, whereas hydrolysable tannins contain ester linkages that are more prone to early thermal cleavage. The high aromatic content and resorcinol-type structures in quebracho tannin favor extensive crosslinking and reticulation reactions upon heating, leading to the formation of a dense and thermally stable char layer. This aromatic carbonaceous residue acts as an efficient physical barrier, limiting heat transfer and the release of flammable volatiles during thermal degradation. As a result, quebracho tannin exhibits both a significantly higher char yield and a reduced heat release, as observed in TGA and PCFC analyses. In contrast, hydrolysable tannins partially decompose through ester bond cleavage and saccharide degradation, which limits their char-forming efficiency despite their relatively high residue content.

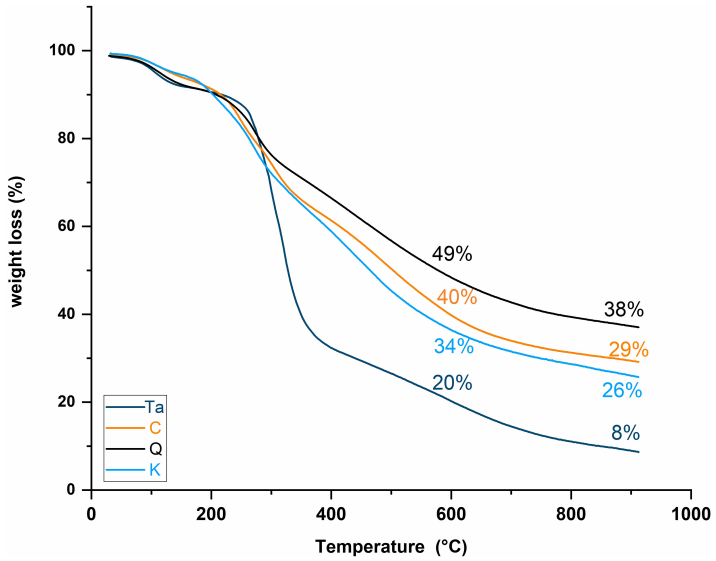

Figure 5: Ta: tannic acid; K: oak tannin; Q: quebracho tannin; C: chestnut tannin at a heating rate of 10°C·min^{-1} under nitrogen atmosphere.

To conclude, condensed tannins exhibit higher char yields at elevated temperatures than hydrolysable tannins, owing to their distinct chemical structures. Condensed tannins are polymers formed by the condensation of multiple flavonoid units, which provide greater thermal stability. In contrast, hydrolysable tannins are composed of phenolic acids esterified to sugar cores; upon heating, these ester bonds are cleaved, leading to the release of sugars and phenolic acids that evaporate or undergo further degradation. The stronger interflavonoid linkages in condensed tannins make them more resistant to thermal decomposition, thus favoring carbonization over volatilization. Consequently, they generate higher char residues during pyrolysis or combustion. Among the samples studied, quebracho tannins produced the highest char yield (49% at 600°C), compared to oak and chestnut tannins (36% and 40% at 600°C, respectively), highlighting their potential as promising bio-based flame-retardant components. The combustibility of the different tannins was then investigated by micro-calorimetry with a pyrolysis combustion flow calorimeter (PCFC). The results are presented in Fig. 6.

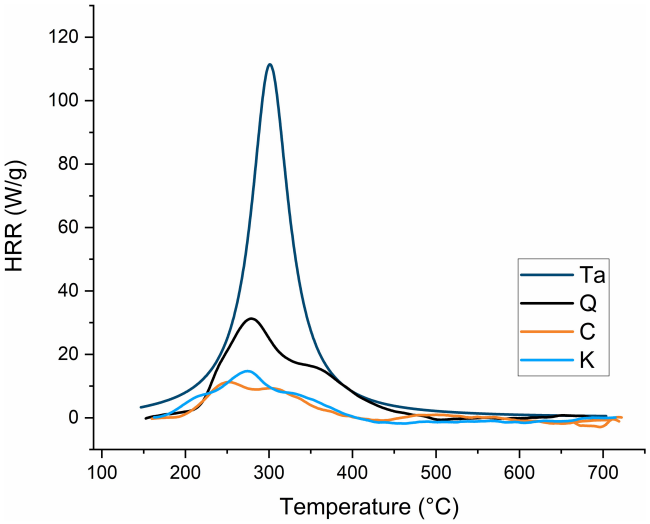

Figure 6: Heat release rate (HRR) curves of the different tannins (Ta: tannic acid; K: oak tannin; Q: quebracho tannin; C: chestnut tannin).

Hydrolysable tannins (Ta, C, and K) release combustible gases over a broad temperature range (150°C–500°C), reflecting their multi-step thermal degradation behavior. Tannic acid (Ta) exhibits the highest flammability among the studied tannins, with a peak heat release rate (pHRR) of 111 $W \cdot g^{-1}$ at 301°C and a total heat release (THR) of approximately 9 kJ. This high pHRR is consistent with its relatively low char yield observed by TGA, indicating limited condensed-phase stabilization.

In contrast, oak (K) and chestnut (C) tannins display much lower pHRR values of 15 $W \cdot g^{-1}$ at 277°C and 11 $W \cdot g^{-1}$ at 247°C, respectively, along with very low THR values (~2.5 kJ). These results are in good agreement with those reported by Karaseva et al. [50], who highlighted the strong influence of tannin composition on microscale fire behavior. The reduced heat release of these tannins is associated with their higher char yields, which limit the amount of combustible volatiles available during pyrolysis.

Condensed quebracho tannin (Q) shows an intermediate pHRR value of 32 $W \cdot g^{-1}$ at 280°C and a THR of approximately 3.2 kJ, with combustible gas release occurring between 210 and 500°C. Although its pHRR is higher than that of oak and chestnut tannins, quebracho tannin produces significantly higher char yields, as evidenced by TGA results. This behavior indicates a more efficient condensed-phase mechanism, where aromatic reticulation and carbonization reduce fuel availability during combustion.

From a microscale fire perspective, these trends suggest an inverse relationship between char yield and heat release capacity (HRC), as materials forming larger amounts of thermally stable char exhibit lower effective combustibility. Tannic acid, characterized by the lowest char yield, presents the highest heat release, whereas quebracho tannin combines moderate heat release with enhanced char formation. This balance between controlled volatile release and efficient condensed-phase stabilization explains the favorable fire performance of quebracho tannin and supports its selection as a promising precursor for further phosphorus-based flame-retardant modification.

The superior thermal performance of quebracho tannin compared to hydrolysable tannins can therefore be directly attributed to its condensed polyflavonoid structure. Unlike hydrolysable tannins, which contain thermally labile ester linkages that undergo early cleavage and volatilization, condensed tannins favor carbonization over volatilization due to their highly aromatic and crosslinked networks. The resulting char layer acts as an efficient physical barrier, limiting heat transfer and the release of flammable volatiles during

thermal degradation. This condensed-phase barrier effect explains both the significantly higher char yield observed in TGA and the reduced heat release measured by PCFC for quebracho tannin.

The chemical structure of quebracho tannin, consisting predominantly of condensed polyflavonoid units linked through C–C interflavonoid bonds, has been extensively reported in the literature [47,53,54]. In this work, this structural description is recalled to support the discussion of its thermal behavior and its reactivity toward phosphorylation.

The combustibility of the different tannins was subsequently investigated using microcalorimetry with a pyrolysis combustion flow calorimeter (PCFC). The corresponding results are presented in Fig. 6.

Inductively coupled plasma (ICP) analysis was used to quantify the phosphorus content of QPHYA and QPHOA (Table 1). As expected, raw quebracho tannins (Q) contained no detectable phosphorus. After phosphorylation, significant P incorporation was observed, with contents of 13.0 ± 0.14% for QPHYA and 15.0 ± 0.12% for QPHOA, confirming successful functionalization. Complementary SEM–EDX analyses (Table 1) provided consistent results, with slightly higher P levels detected in QPHOA compared to QPHYA. Elemental analysis further revealed a marked decrease in carbon content (from 64.9 ± 0.2% in Q to 34.5 ± 0.3% in QPHOA and 47.8 ± 0.2% in QPHYA) and a concomitant increase in oxygen (from 33.8 ± 0.2% in Q to 45.9 ± 0.2% in QPHOA and 41.7 ± 0.2% in QPHYA). These variations are consistent with phosphorylation reactions, where hydroxyl groups of tannins are substituted or crosslinked with phosphorus-containing groups, leading to higher oxygen incorporation and lower relative carbon content.

Table 1: ICP and elemental analysis through SEM-EDX of raw Q tannins and phosphorylated Q tannins with phytic acid (QPHYA) and phosphoric acid (QPHOA).

Samples	SEM-EDX		ICP	
	%C	%O	%P	%P
Q	64.9 ± 0.2	33.8 ± 0.2	–	–
QPHYA	47.8 ± 0.2	41.7 ± 0.2	11.1 ± 0.1	13 ± 0.1
QPHOA	34.5 ± 0.3	45.9 ± 0.2	15.7 ± 0.1	15 ± 0.1

FTIR spectra of raw quebracho tannins (Q) and phosphorylated tannins (QPHYA and QPHOA) are shown in Fig. 7. The characteristic vibrational bands of untreated tannins are present in all samples, but additional peaks appear after phosphorylation. New absorption bands were detected at 1110 cm^{-1} (symmetric P=O(OH) stretching), 1039 cm^{-1} (PO_2 vibrations), and 954 cm^{-1} (symmetric P–O stretching), which are assigned to ester linkages of phosphate groups. A new band at 1710 cm^{-1}, corresponding to C=O stretching of carbonyl groups (ketones, aldehydes), was also observed in QPHYA and QPHOA, indicating phosphorus incorporation and treatment-induced chemical changes in the tannin structure. These features confirm the formation of P–O linkages between phosphate groups and the hydroxyl functionalities of tannins, consistent with phosphorylation by (poly)phosphoric salts. Comparison between the two phosphorylation routes suggests that phosphoric acid is generally more efficient than phytic acid. Its higher reactivity towards hydroxyl groups promotes greater incorporation of phosphorus through phosphate ester formation, while the resulting products tend to exhibit enhanced stability, thereby improving functionalization efficiency.

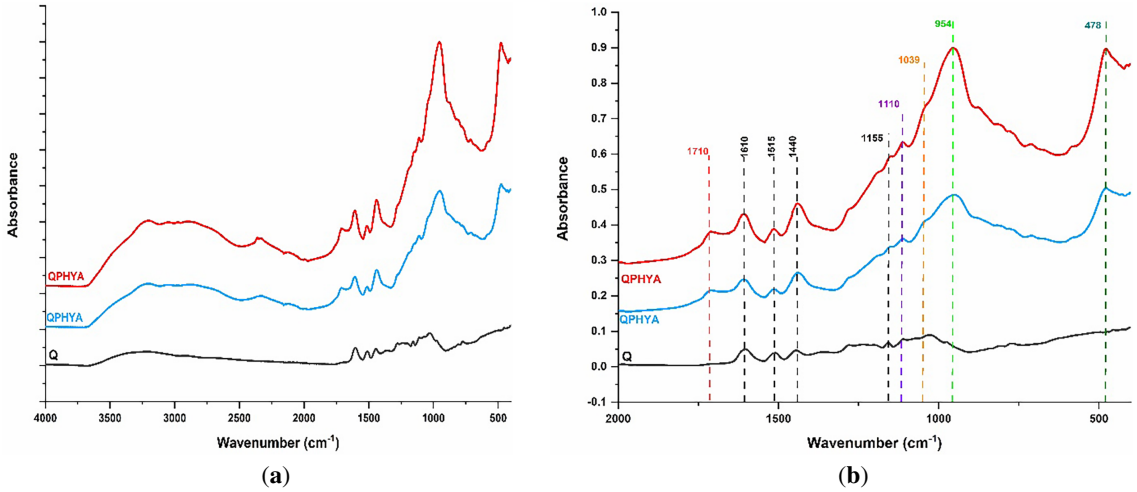

Figure 7: FTIR spectra of raw quebracho tannins (Q, black line) and phosphorylated quebracho tannins QPHYA (blue line) and QPHOA (red line): (**a**) spectral range from 4000 to 400 cm^{-1}; (**b**) zoomed region from 2000 to 400 cm^{-1}.

^{31}P nuclear magnetic resonance (NMR) was used to characterize phosphorus-containing species in phosphorylated tannins QPHYA and QPHOA (Fig. 8). As expected, no signal was observed for raw quebracho tannins (Q), confirming the absence of phosphorus. The QPHYA spectrum displayed a single resonance at ~0 ppm, assigned to PO_4 phosphates and/or PO_4^{3-} phosphate esters, in agreement with literature data [55]. In contrast, the QPHOA spectrum exhibited a main peak at 0 ppm, characteristic of phosphate groups, together with additional resonances at –10, –19, and –20 ppm, which correspond to polyphosphates [55]. The chemical shifts toward negative values are consistent with the highly deacetylated nature of polyphosphate chains, where strong dipolar interactions between neighboring phosphorus atoms influence the local electronic environment. It should be noted, however, that these shifts may vary depending on polyphosphate type and experimental conditions. Based on these chemical characterizations, schematic reaction pathways were proposed for the phosphorylation of quebracho tannins by phytic acid (Fig. 9a) and by phosphoric acid (Fig. 9b). Although FTIR and ^{31}P NMR analyses clearly demonstrate phosphorus incorporation and the formation of P–O-containing species, they do not allow an unambiguous distinction between covalent grafting and strong physical interactions between tannins and phosphate species. Additional analyses would be required to fully elucidate the reaction mechanism.

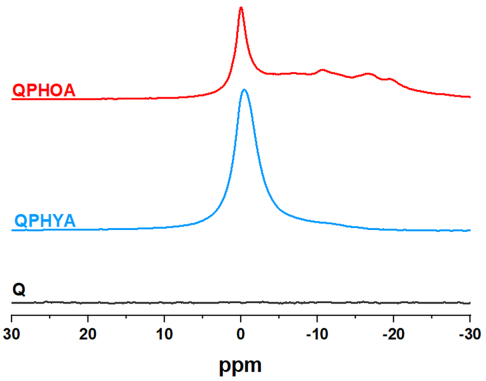

Figure 8: ^{31}P NMR spectra of raw quebracho tannins (Q, black line) and phosphorylated quebracho tannins QPHYA (blue line) and QPHOA (red line).

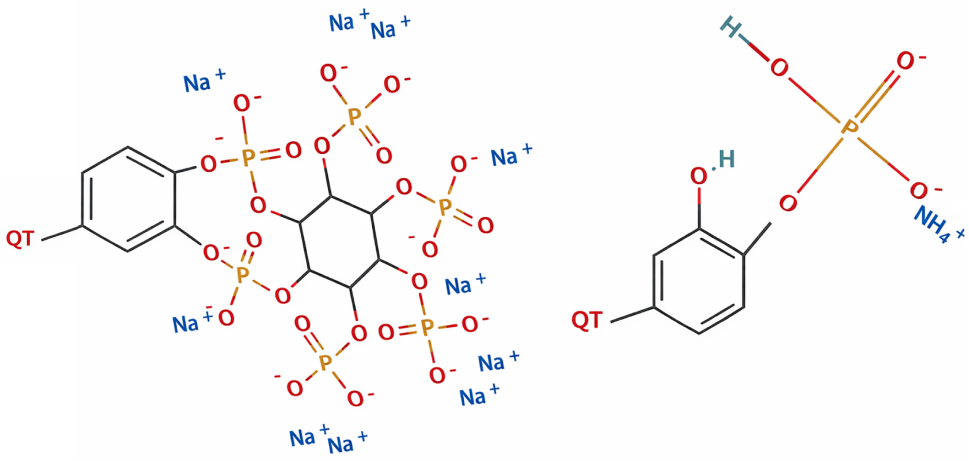

Figure 9: Schematic representation of the potential reactions occurring between quebracho tannins and (**a**) phytic acid and (**b**) phosphoric acid.

The thermal stability of phosphorylated tannins was investigated by thermogravimetric analysis (TGA) under nitrogen (Figs. 10 and 11). The main thermal parameters onset degradation temperature (T_{onset}), maximum degradation temperature (T_{max}), and char yields at 600°C ($Char_{600}$) and 900°C ($Char_{900}$), are summarized in Table 2, along with phosphorus contents determined by ICP. Compared to raw quebracho tannins (Q), phosphorylated tannins (QPHYA and QPHOA) exhibited distinct thermal degradation profiles and significantly higher char residues (44% and 52% at 900°C, compared with 38% for Q). The initial weight loss below 150°C, corresponding to water evaporation, was observed for all samples. However, differences emerged at higher temperatures: while raw Q displayed a single peak at 274°C, phosphorylated tannins showed broader multiple peaks between 150°C–260°C. In addition, the major degradation of flavonoid units shifted from 483°C (Q) to higher temperatures—546°C (QPHYA) and 508°C (QPHOA)-in agreement with observations for phosphorylated lignin [48]. These modifications can be attributed to phosphorus-containing groups, which catalyze dehydration and promote char formation. For phytic acid derivatives, two distinct mass-loss stages were identified (160°C–290°C), consistent with dehydration followed by thermal decomposition [56]. Similar effects were previously reported for phosphorylated tannic acid [57], lignin [48], and lignocellulosic fibers [58]. Overall, the increase in char yield arises from condensation reactions induced by phosphorus, which enhance carbon accumulation at the surface. This protective char layer can swell and act as a thermal barrier, thereby limiting heat transfer to the underlying material. In this study, the combination of quebracho tannins with phosphorus led to a favorable balance: although T_{onset} decreased by ~34%, char formation increased by ~37% at both 600°C and 900°C, confirming the efficiency of phosphorus-based systems as effective charring promoters.

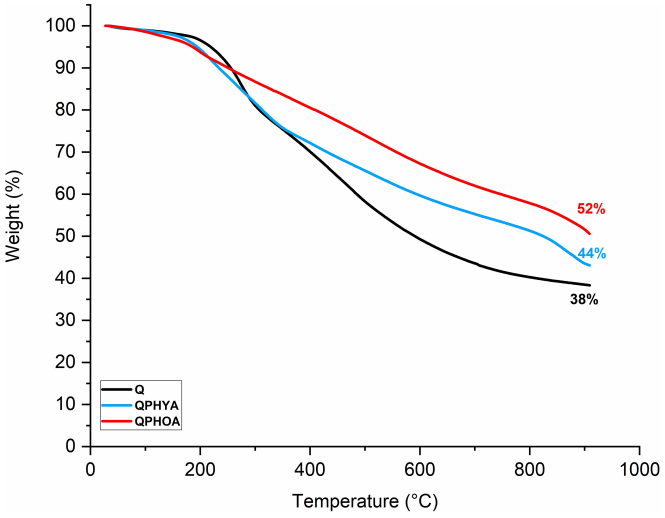

Figure 10: TGA curves of raw (Q) and phosphorylated (QPHYA and QPHOA) condensed quebracho tannins under nitrogen atmosphere.

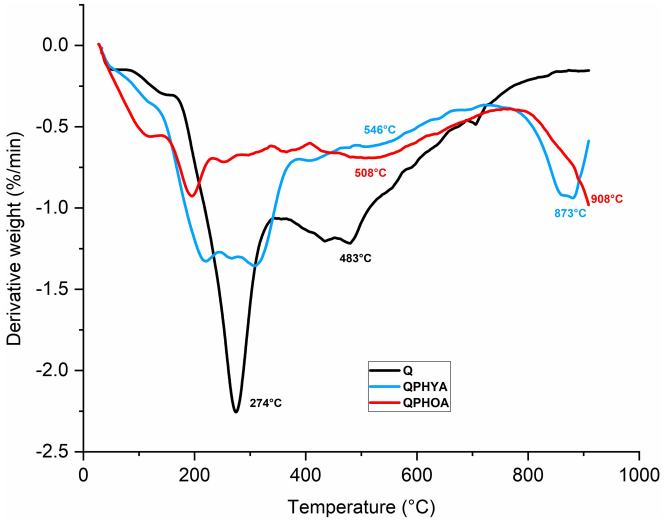

Figure 11: DTG curves of raw (Q) and phosphorylated (QPHYA and QPHOA) quebracho tannins under nitrogen atmosphere.

Table 2: TGA parameters of Q, QPHYA and QPHOA under nitrogen as well as the P content determined by ICP analysis.

Tannins	T_{onset} (°C)	Char600 (%)	Char900 (%)	%P (ICP)
Q	215 ± 2	49 ± 0.5	38 ± 0.4	0
QPHYA	162 ± 3	60 ± 0.4	44 ± 0.5	13 ± 0.1
QPHOA	142 ± 3	67 ± 0.7	52 ± 0.5	15 ± 0.1

The pyrolysis behavior of raw (Q) and phosphorylated tannins (QPHYA and QPHOA) was evaluated by pyrolysis combustion flow calorimetry (PCFC). The heat release rate (HRR) curves (Fig. 12) confirmed the multistep decomposition observed by TGA (Fig. 11), with peak temperatures slightly shifted to higher values due to the higher heating rate applied in PCFC (60°C·min^{-1} compared to 10°C·min^{-1} for TGA). The initial mass loss observed at approximately 100°C in TGA could not be detected in PCFC, as water vapor does not contribute to heat release. Raw quebracho tannin exhibited a main HRR peak at approximately 280°C, followed by a shoulder near 355°C and a gradual decline up to 500°C. In contrast, phosphorus-treated samples showed a marked modification of the pyrolysis profile. QPHYA displayed an early HRR peak at 167°C, a second peak at 310°C, and a major contribution around 715°C. QPHOA showed a delayed heat release, with a sharp HRR increase above 650°C and a poorly defined maximum beyond 700°C. Due to the upper temperature limit of PCFC (750°C), decomposition at higher temperatures could not be fully resolved, although DTG results confirmed ongoing degradation of phosphorus-treated samples up to 900°C.

These results indicate that phosphorus-containing species modify the thermal degradation pathway and shift part of the heat release toward higher temperatures, reflecting changes in decomposition kinetics rather than enhanced carbonization of the organic matrix. More importantly, phosphorylation of quebracho tannins leads to higher solid residues, with QPHYA and QPHOA exhibiting char yields of 60% and 67% at 600°C, and 44% and 52% at 900°C, respectively. However, this increase in residue cannot be unambiguously attributed to enhanced carbonization of the organic tannin structure. As discussed above, the additional char yield mainly originates from the thermally stable inorganic phosphate fraction remaining in the condensed phase during thermal degradation.

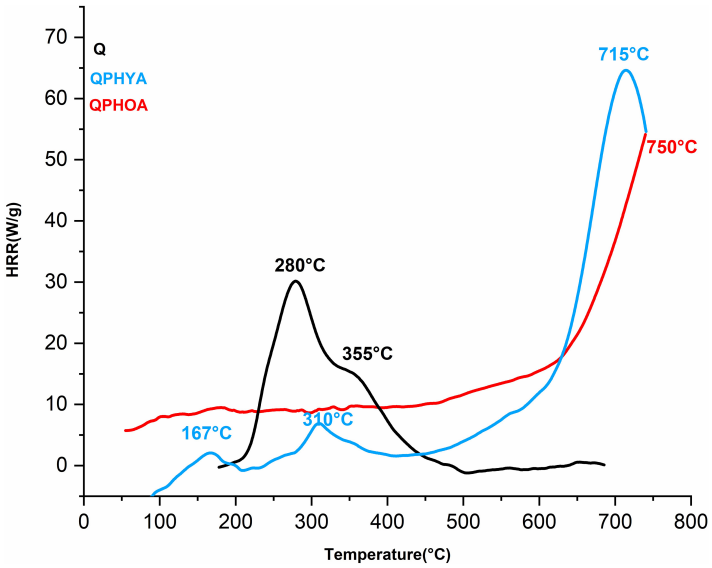

Figure 12: PCFC curves of raw (Q) and phosphorylated (QPHYA and QPHOA) condensed quebracho tannins.

Overall, the present results demonstrate that phosphorus incorporation alters the pyrolysis behavior of quebracho tannins and increases the amount of solid residue due to the retention of inorganic phosphate species. Further investigations, including detailed mass balance analyses of organic vs. inorganic contributions, would be required to conclusively assess any enhancement of intrinsic carbonization.

To better contextualize these results, a comparison with literature data on phosphorus-modified bio-based materials is presented below. These observations are consistent with previous studies reporting the effect of phosphorus-based modifications on the thermal degradation of polyphenolic compounds and

bio-based polymers. In particular, phosphorus-containing groups are known to promote dehydration, crosslinking, and rearrangement reactions at relatively low temperatures, which can lead to an early heat release followed by stabilization of the condensed phase at higher temperatures [59]. Similar multistep pyrolysis behaviors, characterized by early degradation events and delayed heat release at elevated temperatures, have been reported for phosphorylated lignin, tannin-based resins, and other phosphorus-modified biopolymers analyzed by PCFC or cone calorimetry.

Moreover, the shift of HRR contributions toward higher temperatures observed for QPHYA and QPHOA is in line with literature describing a flame-retardant action dominated by condensed-phase mechanisms rather than gas-phase inhibition [60,61]. Several authors have shown that inorganic phosphate species remain thermally stable over a wide temperature range and contribute significantly to the final residue, thereby increasing the apparent char yield without necessarily enhancing the intrinsic carbonization of the organic matrix [62]. This behavior has been particularly highlighted for ammonium polyphosphate–treated systems, where the residual mass is largely associated with phosphate-rich inorganic structures rather than aromatic carbonaceous char [63].

Consequently, the present results corroborate literature findings indicating that phosphorus incorporation primarily modifies degradation kinetics and residue composition. While the increased char yields partly reflect the persistence of inorganic phosphate species in the condensed phase, this behavior remains highly relevant from a flame-retardant perspective, as the formation of thermally stable residues effectively limits heat release and material degradation.

To highlight the potential of phosphorylated tannins as sustainable flame retardants, their thermal behavior was compared with that of conventional phosphorus-based flame retardants commonly used in polymeric systems. Typically, commercial phosphorus additives such as ammonium polyphosphate (APP) or aluminium phosphinate (AlPi) exhibit onset degradation temperatures (T_{onset}) between 250°C–320°C and generate moderate char yields of ~20%–35% at 600°C, depending on the polymer matrix [10,64]. Aryl phosphate esters such as triphenyl phosphate (TPP) or resorcinol bis(diphenyl phosphate) (RDP) generally show even lower char yields (≤15%) under similar conditions, reflecting their volatilization-dominated mechanism of action [3]. In addition, cyclic phosphates such as DOPO (9,10-dihydro-9-oxa-10-phosphaphenanthrene-10-oxide) and chlorinated organophosphates including tris(2-chloroethyl) phosphate (TCEP) and tris(2-chloroisopropyl) phosphate (TCPP) are widely employed as efficient gas-phase flame inhibitors. However, they typically produce limited condensed-phase residues (≤20%) because of partial volatilization and cleavage of P–C or P–O bonds during degradation [65–67]. In contrast, the condensed quebracho tannins investigated here demonstrated higher intrinsic char formation (49% at 600°C, 38% at 900°C) compared to most commercial phosphorus-based systems. More importantly, phosphorylation of quebracho tannins markedly improved this behavior, with QPHYA and QPHOA exhibiting char yields of 60% and 67% at 600°C, and 44% and 52% at 900°C, respectively. Although their Tonset values (162°C for QPHYA and 142°C for QPHOA) are lower than those of conventional additives, the significant increase in char formation, well above values typically reported for commercial phosphorus compounds demonstrates their efficiency as charring promoters. These findings underline the competitive performance of phosphorylated tannins, while offering the additional advantage of being fully bio-based, and derived from renewable wood resources, thus positioning them as promising sustainable alternatives to commercially available phosphorus flame retardants. Therefore, the phosphorus incorporated into tannin molecules acts primarily in the condensed phase by promoting char formation, rather than through volatilization as observed for low-molecular-weight phosphorus additives.

Moreover, the phosphorylation process developed in this study involves mild, aqueous conditions and readily available reagents, making it easily scalable and compatible with industrial processing routes for bio-based composites.

3.2 Impregnation of Flax Fibers with Phosphorus-Modified Tannins

Rovings treated using the impregnation line exhibited higher dry pick-up rates (Δ%), regardless of the solution used (Table 3). Phosphorylated tannins consistently improved impregnation efficiency compared to their non-phosphorylated counterparts, with TR-QPHOA5N1 showing the highest Δ%. This behavior can be attributed to the continuous fiber structure of rovings, which promotes deeper molecular diffusion and more efficient impregnation.

Table 3: The pick-up rate of rovings.

Process	Structure	Δ%
Impregnation line	TRQ5N1	16.14 ± 1.25
	TRQPHYA5N1	18.33 ± 3.74
	TRQPHO5N1	17.76 ± 4.22

The impregnation efficiency of phosphorylated tannins (QPHYA and QPHOA) onto flax fibers was assessed by ICP, SEM–EDX, and FTIR analyses. ICP quantification confirmed significant phosphorus incorporation in the treated rovings, reaching 3.7 ± 0.3 wt.% for QPHOA and 1.8 ± 0.1 wt.% for QPHYA, consistent with their impregnation capacity (Table 4).

Table 4: ICP analysis of flax rovings treated with phosphorylated tannins.

Samples	% P (ICP)
UR	Not Detected
TRQPHYA5N1	1.8 ± 0.1
TRQPHOA5N1	3.7 ± 0.3

SEM–EDX mapping further revealed a preferential localization of phosphorus at the fiber surfaces, with higher contents for TR-QPHOA. FTIR spectra confirmed the successful impregnation of phosphorus groups, showing new absorption bands at ~1240–1020 cm^{-1} (P=O, P–OH, and P–O–C) and characteristic tannin peaks (C=C aromatic and C–O), indicating effective interactions between phosphorus-modified tannin systems and flax fibers [54,68]. Phosphorus distribution was analyzed by SEM–EDX on flax roving cross-sections (Fig. 13). In both treatments, phosphorus was mainly detected at the surface of elementary fibers, with decreasing concentration toward the core. In agreement with ICP results, TR-QPHOA5N1 exhibited a higher phosphorus content (≈4 wt.%) than TR-QPHYA5N1 (≈2 wt.%).

FTIR spectra were obtained for flax rovings treated with phosphorylated quebracho tannins (TRQ-PHYA5N1 and TRQPHOA5N1) and compared with untreated controls (Fig. 14). Treated fibers exhibited new absorption bands typical of phosphorus-containing groups, including ~1710 cm^{-1} (C=O stretching), 1240 and 1020 cm^{-1} (P=O and P–OH), and 870–720 cm^{-1} (P–O–C vibrations) [61]. These features confirm the formation of cross-links between phosphorus and cellulose, demonstrating successful phosphorylation of flax fibers. Such interactions likely involve hydroxyl, ether, or ester groups of cellulose [5]. Furthermore, TR-Q5N1 spectra showed peaks at 1610 and 1510 cm^{-1} (C=C aromatic stretching) and 1420 cm^{-1} (C–O and O–H), confirming the presence of tannin moieties.

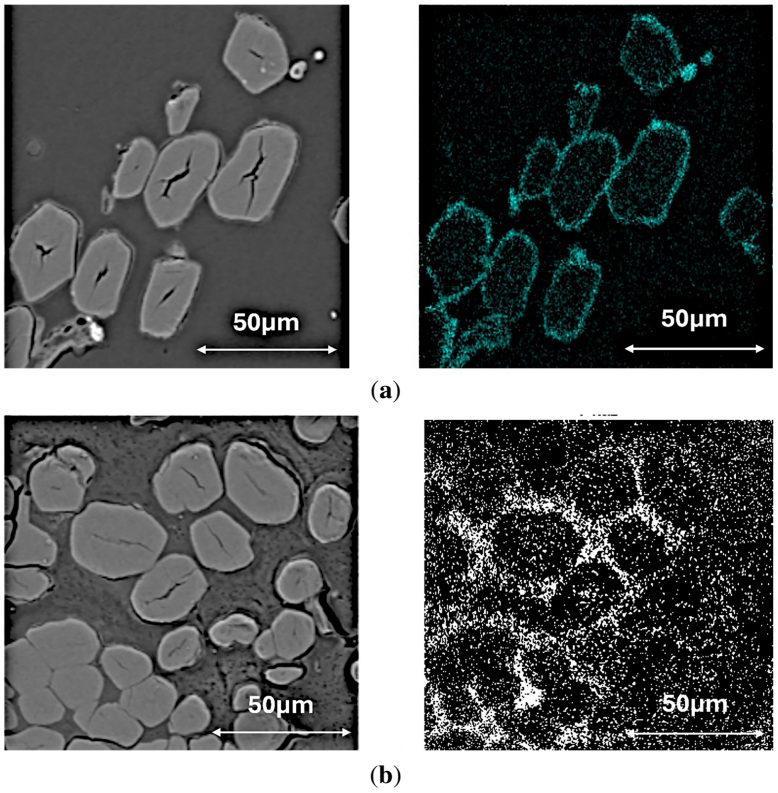

Figure 13: SEM micrographs (left) and EDX phosphorus elemental maps (right) of flax rovings treated with (**a**) TR-QPHYA5N1 and (**b**) TR-QPHOA5N1, showing the surface distribution of phosphorus after treatment.

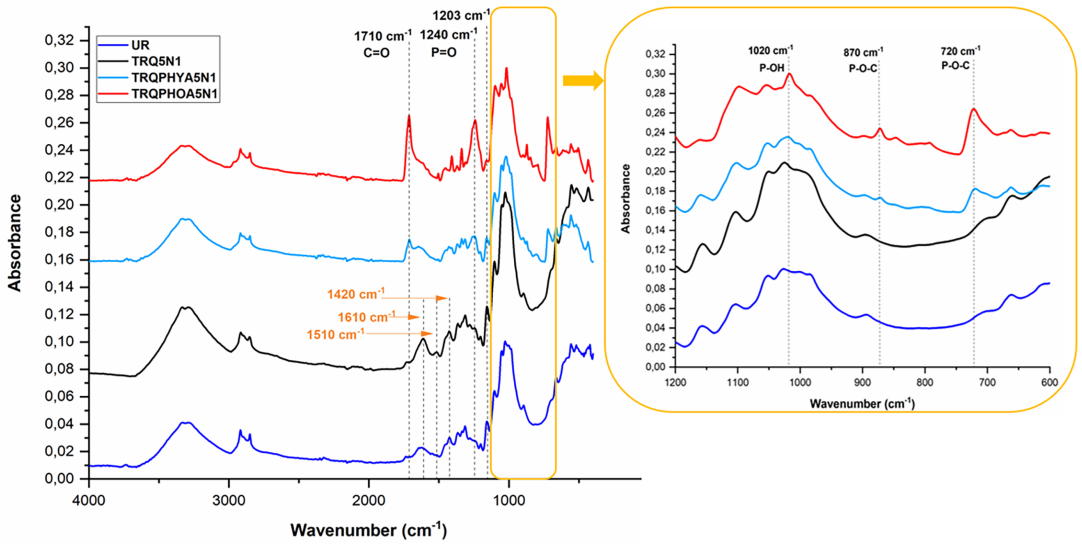

Figure 14: FTIR-ATR spectra of untreated flax rovings, those treated with phosphorylated tannin formulations and raw tannins.

Fig. 15 shows the TGA curves of untreated flax rovings and those chemically modified with non-phosphorylated and phosphorylated quebracho tannins. The main thermal parameters are summarized in Table 5.

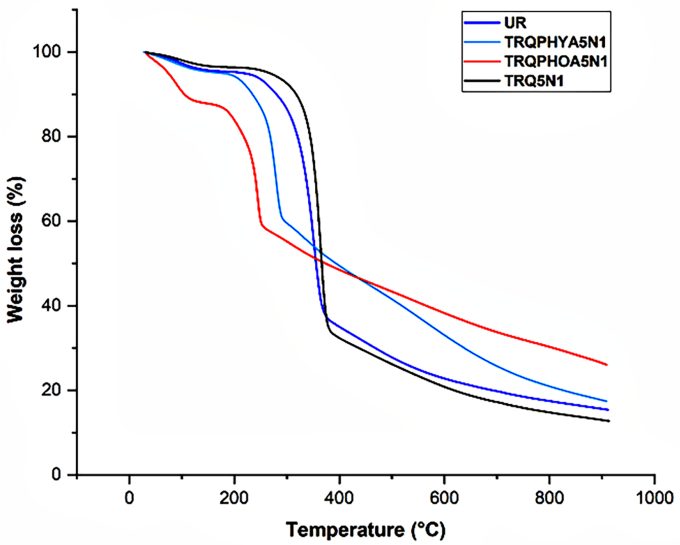

Figure 15: Thermogravimetric (TGA) curves under nitrogen atmosphere of untreated flax rovings (UR), non-phosphorylated tannin-treated fibers (TRQ5N1), and phosphorylated tannin-treated fibers (TRQPHYA5N1 and TRQPHOA5N1).

Table 5: Main thermal degradation parameters obtained from TGA under nitrogen for untreated (UR), non-phosphorylated (TRQ5N1), and phosphorylated flax rovings (TRQPHYA5N1, TRQPHOA5N1).

	T_{onset} °C	T_{max} °C	% Mass of Residue at 600°C	% Mass of Residue at 900°C
UR	320 ± 2	356 ± 2	23 ± 1	16 ± 2
TRQ5N1	337 ± 3	365 ± 2	21 ± 2	13 ± 2
TRQPHYA5N1	258 ± 1	279 ± 3	33 ± 2	22 ± 3
TRQPHOA5N1	223 ± 4	246 ± 2	38 ± 1	26 ± 3

The thermal degradation of flax occurs in several successive stages associated with the decomposition of hemicellulose, cellulose, and lignin. The initial weight loss observed around 100°C corresponds to moisture evaporation, followed by the degradation of hemicellulose, waxes, and pectins between 200°C–330°C, and finally cellulose and lignin decomposition between 340°C–500°C [61,62].

The incorporation of tannins significantly altered the thermal response of flax rovings. Samples treated with non-phosphorylated quebracho tannins (TRQ5N1) exhibited delayed degradation compared to untreated flax (UR), with TRQ5N1 showing slightly higher stability (T_{max} = 365°C).

Conversely, rovings treated with phosphorylated tannins (TRQPHYA5N1, TRQPHOA5N1) displayed lower onset and maximum degradation temperatures, indicating an apparent reduction in thermal stability. However, these samples produced markedly higher char yields (33%–38%) than TRQ5N1 (21%), consistent with the well-established charring mechanism of phosphorus-based flame retardants, which promote carbonization through phosphoric acid formation and cellulose phosphorylation. Overall, these findings

confirm that phosphorus content is the key parameter governing the thermal stability and char-forming ability of treated flax rovings.

4 Conclusions

This study investigated the structure, thermal behavior, and microscale fire performance of different tannin types, including hydrolysable tannins (tannic acid, oak, and chestnut) and condensed quebracho tannin. FTIR analysis confirmed their classification within hydrolysable and condensed tannin families, while TGA revealed marked differences in thermal degradation behavior. Among the investigated tannins, quebracho tannin exhibited the highest intrinsic char yield (≈38 wt.% at 900°C) and the lowest heat release parameters determined by PCFC, highlighting its superior condensed-phase behavior and justifying its selection for further modification. Quebracho tannin was subsequently modified using phytic acid (QPHYA) and phosphoric acid (QPHOA). Elemental analyses (ICP and SEM–EDX) confirmed effective phosphorus incorporation, with phosphorus contents of approximately 13 wt.% for QPHYA and 15 wt.% for QPHOA. FTIR and 31P NMR analyses evidenced the presence of phosphate- and phosphate-ester-related species, while additional polyphosphate structures were detected for QPHOA. Phosphorylation significantly altered the thermal degradation pathway and increased solid residue formation, with QPHOA reaching char yields of approximately 52 wt.% at 900°C. However, this increase in residue is mainly attributed to the retention of thermally stable inorganic phosphate species and cannot be unambiguously assigned to enhanced carbonization of the organic tannin matrix. A direct comparison with physical mixtures of tannin and phosphoric or phytic acids was not carried out in this study. Such an investigation would represent a relevant perspective for future work, as it would help to better distinguish the purely physical effects from those induced by the treatment in the observed flame-retardant behavior. Phosphorylated quebracho tannins were further applied to flax rovings to assess their potential as bio-based flame-retardant systems for fiber reinforcements. The treated rovings incorporated significant phosphorus contents (up to 3.7 wt.% for QPHOA) and exhibited enhanced thermal stability, with char yields reaching approximately 38% at 600°C and 26% at 900°C. FTIR analysis indicated the presence of phosphorus-containing functionalities associated with cellulose, supporting effective interfacial interactions between phosphorus-modified tannin systems and flax fibers. Overall, this work demonstrates the potential of phosphorylated quebracho tannins as sustainable flame-retardant precursors, combining high solid residue formation with favorable microscale fire behavior. The study provides a comparative structure–property framework for understanding tannin-based flame-retardant systems and highlights the relevance of condensed tannins for condensed-phase fire protection strategies. Macroscopic flame-resistance tests such as LOI or UL-94 were not performed in this study. While such tests would be valuable for practical assessment, the present work focuses on microscale thermal and combustion analyses as a first screening of flame-retardant potential. Future investigations will address large-scale fire performance, durability, and composite integration to further assess industrial applicability.

Acknowledgement: The authors are indebted to Tristan Mathieu from Terre de Lin Co. (Saint-Pierre-le-Viger, France) for providing the wrapped flax rovings with cotton used in this study. The authors gratefully acknowledge Jean-Claude Roux (IMT Mines Alès) for his technical assistance with scanning electron microscopy (SEM) imaging and Romain Ravel (IMT Mines Alès) for his support with ICP analyses.

Funding Statement: This research received no external funding.

Author Contributions: The authors confirm contribution to the paper as follows: conceptualization, A. Bergeret; methodology, A. Bergeret, D. Perrin, C. Lacoste, and K. Tilouche-Guerdelli; investigation, K. Tilouche-Guerdelli; resources, K. Tilouche-Guerdelli; writing—original draft preparation, K. Tilouche-Guerdelli; writing—review and

editing, D. Perrin, C. Lacoste, and A. Bergeret; visualization, K. Tilouche-Guerdelli; supervision, D. Perrin, C. Lacoste, and A. Bergeret; project administration, C. Lacoste; funding acquisition, A. Bergeret. All authors reviewed and approved the final version of the manuscript.

Data Availability Statement: The data that support the findings of this study are available from the corresponding author Dr. C. Lacoste, upon reasonable request.

Ethics Approval: Not applicable.

Conflicts of Interest: The authors declare no conflicts of interest.

References

1. Directorate General for Civil Security and Crisis. Statistics of fire and rescue services in France. 2025 [cited 2026 Jan 1]. Available from: https://www.interieur.gouv.fr/documentation/etudes-et-statistiques/statistiques-2024-dgscgc.html.
2. Singh I, Sivaramakrishna A. Phosphorus-based polymeric flame retardants-recent advances and perspectives. Chem Sel. 2024;9(26):e202401485. doi:10.1002/slct.202401485.
3. Sonnier R, Taguet A, Ferry L, Lopez-Cuesta JM. Towards bio-based flame retardant polymers. Berlin/Heidelberg, Germany: Springer; 2018. doi:10.1007/978-3-319-67083-6.
4. Chen M, Guo Q, Yuan Y, Li A, Lin B, Xiao Y, et al. Recent advancements of bio-derived flame retardants for polymeric materials. Polymers. 2025;17(2):249. doi:10.3390/polym17020249.
5. Basso MC, Pizzi A, Polesel Maris J, Delmotte L, Colin B, Rogaume Y. MALDI-TOF, ^{13}C NMR and FTIR analysis of the cross-linking reaction of condensed tannins by triethyl phosphate. Ind Crops Prod. 2017;95:621–31. doi:10.1016/j.indcrop.2016.11.031.
6. Quan Y, Zhang W, Marquez JAD, Guo L, Tanchak R, Shen R. Sustainable biomass-based flame retardants: recent advances in starch, phytic acid, and chitosan systems for polymeric materials. Emerg Manage Sci Technol. 2025;5:e016.
7. Hollingbery LA, Hull TR. The fire retardant behaviour of huntite and hydromagnesite—A review. Polym Degrad Stab. 2010;95(12):2213–25. doi:10.1016/j.polymdegradstab.2010.08.019.
8. Lei Y, Zhao X, Xu L, Li H, Liang J, Yeoh GH, et al. Natural flame retardant minerals for advanced epoxy composites. Fire. 2024;7(9):308. doi:10.3390/fire7090308.
9. Morsy A, Kandil S, Ewais HA, Abdel-Salam AH, Mohamed A. Eco-conscious flame retardants for enhanced fire resistance in natural fiber reinforced polymers composite: a review bio-based, and industry implications. Chemosphere. 2025;377:144360. doi:10.1016/j.chemosphere.2025.144360.
10. Nazir R, Gaan S. Recent developments in P(O/S)–N containing flame retardants. J Appl Polym Sci. 2020;137:47910. doi:10.1002/app.47910.
11. Costes L, Laoutid F, Brohez S, Dubois P. Bio-based flame retardants: when nature meets fire protection. Mater Sci Eng R Rep. 2017;117:1–25. doi:10.1016/j.mser.2017.04.001.
12. Wang M, Yin GZ, Yang Y, Fu W, Palencia JLD, Zhao J, et al. Bio-based flame retardants to polymers: a review. Adv Ind Eng Polym Res. 2023;6(2):132–55. doi:10.1016/j.aiepr.2022.07.003.
13. Yuan Q, Wang S, He L, Xu S. Advances in the study of flame-retardant cellulose and its application in polymers: a review. Polymers. 2025;17(9):1249.
14. Fox DM, Temburni S, Novy M, Flynn L, Zammarano M, Kim YS, et al. Thermal and burning properties of poly(lactic acid) composites using cellulose-based intumescing flame retardants. In: Fire and polymers VI: New advances in flame retardant chemistry and science. Washington, DC, USA: American Chemical Society; 2012. p. 223–34. doi:10.1021/bk-2012-1118.ch016.
15. Li M, Prabhakar MN, Park JK, Song JI. Flame-retardant innovations in bio-based treatments for lignocellulosic natural fibers: a review. Int J Biol Macromol. 2025;311:143728. doi:10.1016/j.ijbiomac.2025.143728.
16. Özer MS, Gaan S. Recent developments in phosphorus based flame retardant coatings for textiles: synthesis, applications and performance. Prog Org Coat. 2022;171:107027. doi:10.1016/j.porgcoat.2022.107027.

17. Dorez G, Ferry L, Sonnier R, Taguet A, Lopez-Cuesta JM. Effect of cellulose, hemicellulose and lignin contents on pyrolysis and combustion of natural fibers. J Anal Appl Pyrolysis. 2014;107:323–31. doi:10.1016/j.jaap.2014.03.017.
18. Patwardhan PR, Brown RC, Shanks BH. Product distribution from the fast pyrolysis of hemicellulose. ChemSusChem. 2011;4(5):636–43. doi:10.1002/cssc.201000425.
19. Hu Y, Ye Y, Wang J, Zhang T, Jiang S, Han X. Functionalization of chitosan and its application in flame retardants: a review. Int J Biol Macromol. 2025;295:139615. doi:10.1016/j.ijbiomac.2025.139615.
20. Lu Y, Zhao P, Chen Y, Huang T, Liu Y, Ding D, et al. A bio-based macromolecular phosphorus-containing active cotton flame retardant synthesized from starch. Carbohydr Polym. 2022;298:120076. doi:10.1016/j.carbpol.2022.120076.
21. Wang J, Ren Q, Zheng W, Zhai W. Improved flame-retardant properties of poly(lactic acid) foams using starch as a natural charring agent. Ind Eng Chem Res. 2014;53(4):1422–30. doi:10.1021/ie403041h.
22. Cayla A, Rault F, Giraud S, Salaün F, Fierro V, Celzard A. PLA with intumescent system containing lignin and ammonium polyphosphate for flame retardant textile. Polymers. 2016;8(9):331. doi:10.3390/polym8090331.
23. Ecochard Y, Decostanzi M, Negrell C, Sonnier R, Caillol S. Cardanol and eugenol based flame retardant epoxy monomers for thermostable networks. Molecules. 2019;24(9):1818. doi:10.3390/molecules24091818.
24. Niranjana VS, Ponnan S, Mukundan A, Prabu AA, Wang HC. Emerging trends in silane-modified nanomaterial–polymer nanocomposites for energy harvesting applications. Polymers. 2025;17(10):1416. doi:10.3390/polym17101416.
25. Li Y, Niu HX, Jiang HR, Ma C, Yan Y, Shi HJ, et al. Cardanol-derived phosphorus-containing acrylates as UV-curable, highly transparent and flame retardant coatings for polycarbonate. Ind Crops Prod. 2025;233:121386. doi:10.1016/j.indcrop.2025.121386.
26. Antoun K, Ayadi M, El Hage R, Nakhl M, Sonnier R, Gardiennet C, et al. Renewable phosphorous-based flame retardant for lignocellulosic fibers. Ind Crops Prod. 2022;186:115265. doi:10.1016/j.indcrop.2022.115265.
27. Nam S, Condon BD, Xia Z, Nagarajan R, Hinchliffe DJ, Madison CA. Intumescent flame-retardant cotton produced by tannic acid and sodium hydroxide. J Anal Appl Pyrolysis. 2017;126:239–46. doi:10.1016/j.jaap.2017.06.003.
28. Mukherjee S, Uddin KMA, Turku I, Rohumaa A, Lipponen J. Bio-based flame retardants derived from forest industry—An approach towards circular economy. Resour Environ Sustain. 2025;21:100229. doi:10.1016/j.resenv.2025.100229.
29. Korey M, Johnson A, Webb W, Dietenberger M, Youngblood J, Howarter J. Tannic acid-based prepolymer systems for enhanced intumescence in epoxy thermosets. Green Mater. 2020;8(3):150–61. doi:10.1680/jgrma.19.00061.
30. Shan S, Ji W, Zhang S, Huang Y, Yu Y, Yu W. Insights into the immobilization mechanism of tannic acid on bamboo cellulose fibers. Ind Crops Prod. 2022;182:114836. doi:10.1016/j.indcrop.2022.114836.
31. Zhang AN, Zhao HB, Cheng JB, Li ME, Li SL, Cao M, et al. Construction of durable eco-friendly biomass-based flame-retardant coating for cotton fabrics. Chem Eng J. 2021;410:128361. doi:10.1016/j.cej.2020.128361.
32. Kim YO, Cho J, Yeo H, Lee BW, Moon BJ, Ha YM, et al. Flame retardant epoxy derived from tannic acid as biobased hardener. ACS Sustainable Chem Eng. 2019;7(4):3858–65. doi:10.1021/acssuschemeng.8b04851.
33. Xia Z, Singh A, Kiratitanavit W, Mosurkal R, Kumar J, Nagarajan R. Unraveling the mechanism of thermal and thermo-oxidative degradation of tannic acid. Thermochim Acta. 2015;605:77–85. doi:10.1016/j.tca.2015.02.016.
34. Pizzi A. Recent developments in eco-efficient bio-based adhesives for wood bonding: opportunities and issues. J Adhes Sci Technol. 2006;20(8):829–46. doi:10.1163/156856106777638635.
35. Hemingway RW. Introduction to the chemistry and significance of condensed tannins. J Eng Appl Sci. 1996;2:1382–6. doi:10.1007/978-1-4684-7511-1.
36. Lisperguer J, Saravia Y, Vergara E. Structure and thermal behavior of tannins from *Acacia dealbata* bark and their reactivity toward formaldehyde. J Chil Chem Soc. 2016;61(4):3188–90. doi:10.4067/s0717-97072016000400007.
37. Wang X, Yang G, Guo H. Tannic acid as biobased flame retardants: a review. J Anal Appl Pyrolysis. 2023;174:106111. doi:10.1016/j.jaap.2023.106111.
38. Cheng XW, Guan JP, Tang RC, Liu KQ. Phytic acid as a bio-based phosphorus flame retardant for poly(lactic acid) nonwoven fabric. J Clean Prod. 2016;124:114–9. doi:10.1016/j.jclepro.2016.02.113.

39. Liu Y, Zhang A, Cheng Y, Li M, Cui Y, Li Z. Recent advances in biomass phytic acid flame retardants. Polym Test. 2023;124:108100. doi:10.1016/j.polymertesting.2023.108100.
40. Karaseva V, Bergeret A, Lacoste C, Fulcrand H, Ferry L. New biosourced flame retardant agents based on Gallic and ellagic acids for epoxy resins. Molecules. 2019;24(23):4305. doi:10.3390/molecules24234305.
41. Bifulco A, Malucelli G. Phytic acid and its derivatives as valuable flame retardants for polymer systems: current state of the art and perspectives. Polymers. 2026;18(6):671. doi:10.3390/polym18060671.
42. Sykam K, Försth M, Sas G, Restás Á, Das O. Phytic acid: a bio-based flame retardant for cotton and wool fabrics. Ind Crops Prod. 2021;164:113349. doi:10.1016/j.indcrop.2021.113349.
43. Kulkarni S, Xia Z, Yu S, Kiratitanavit W, Morgan AB, Kumar J, et al. Bio-based flame-retardant coatings based on the synergistic combination of tannic acid and phytic acid for nylon–cotton blends. ACS Appl Mater Interfaces. 2021;13(51):61620–8. doi:10.1021/acsami.1c16474.
44. Marques JF, Baldissera AF, Silveira MR, Dornelles AC, Ferreira CA. Performance of phosphorylated tannin-based intumescent coatings in passive fire protection. J Coat Technol Res. 2021;18(3):899–910. doi:10.1007/s11998-020-00440-2.
45. Mohamed A, Thyab RM, Ewais HA, Morsy A, Kamel HM, Salem A, et al. Bio-fiber reinforced high-density polyethylene composites—A sustainable approach to improve flame retardancy, biodegradation, and water resistance. J Thermoplast Compos Mater. 2025;29:089270572513610. doi:10.1177/08927057251397836.
46. Falcão L, Araújo MEM. Application of ATR-FTIR spectroscopy to the analysis of tannins in historic leathers: the case study of the upholstery from the 19th century Portuguese Royal Train. Vib Spectrosc. 2014;74:98–103. doi:10.1016/j.vibspec.2014.08.001.
47. Arbenz A, Avérous L. Chemical modification of tannins to elaborate aromatic biobased macromolecular architectures. Green Chem. 2015;17(5):2626–46. doi:10.1039/c5gc00282f.
48. Carretier V, Pucci MF, Lacoste C, Regazzi A, Lopez-Cuesta JM. An efficient solution to determine surface energy of powders and porous media: application to untreated and treated lignin. Appl Surf Sci. 2022;579:152159. doi:10.1016/j.apsusc.2021.152159.
49. Tilouche-Guerdelli K, Lacoste C, Perrin D, Liotier PJ, Ouagne P, Tirillò J, et al. Tannins as biobased molecules for surface treatments of flax wrapped rovings for epoxy/flax fabrics biocomposites: influence on mechanical properties through a multi-scale approach. J Compos Sci. 2024;8(2):75. doi:10.3390/jcs8020075.
50. Karaseva V, Bergeret A, Lacoste C, Ferry L, Fulcrand H. Influence of extraction conditions on chemical composition and thermal properties of chestnut wood extracts as tannin feedstock. ACS Sustainable Chem Eng. 2019;7(20):17047–54. doi:10.1021/acssuschemeng.9b03000.
51. Poletto M. Effect of extractive content on the thermal stability of two wood species from Brazil. Maderas Cienc Y Tecnol. 2016;18(3):435–42. doi:10.4067/S0718-221X2016005000039.
52. Konai N, Raidandi D, Pizzi A, Girods P, Lagel MC, Kple M. Thermogravimetric analysis of anningre tannin resin. Maderas Cienc Y Tecnol. 2016;18(2):245–52. doi:10.4067/S0718-221X2016005000022.
53. Pizzi A. Tannins: prospectives and actual industrial applications. Biomolecules. 2019;9(8):344. doi:10.3390/biom9080344.
54. Venter PB, Sisa M, van der Merwe MJ, Bonnet SL, van der Westhuizen JH. Analysis of commercial proanthocyanidins. Part 1: the chemical composition of quebracho (*Schinopsis lorentzii* and *Schinopsis balansae*) heartwood extract. Phytochemistry. 2012;73:95–105. doi:10.1016/j.phytochem.2011.10.006.
55. Khodavandegar S, Fatehi P. Phytic acid derivatized lignin as a thermally stable and flame retardant material. Green Chem. 2024;26(19):10070–86. doi:10.1039/d4gc03169e.
56. Daneluti ALM, do Rosário Matos J. Study of thermal behavior of phytic acid. Braz J Pharm Sci. 2013;49(2):275–83. doi:10.1590/s1984-82502013000200009.
57. Laoutid F, Karaseva V, Costes L, Brohez S, Mincheva R, Dubois P. Novel bio-based flame retardant systems derived from tannic acid. J Renew Mater. 2018;6(7):559–72. doi:10.32604/jrm.2018.00004.
58. Hajj R, El Hage R, Sonnier R, Otazaghine B, Rouif S, Nakhl M, et al. Influence of lignocellulosic substrate and phosphorus flame retardant type on grafting yield and flame retardancy. React Funct Polym. 2020;153:104612. doi:10.1016/j.reactfunctpolym.2020.104612.

59. Alongi J, Han Z, Bourbigot S. Intumescence: tradition versus novelty. A comprehensive review. Prog Polym Sci. 2015;51:28–73. doi:10.1016/j.progpolymsci.2015.04.010.
60. Illy N, Couture G, Auvergne R, Caillol S, David G, Boutevin B. New prospects for the synthesis of N-alkyl phosphonate/phosphonic acid-bearing oligo-chitosan. RSC Adv. 2014;4(46):24042–52. doi:10.1039/c4ra02501f.
61. Asim M, Paridah MT, Chandrasekar M, Shahroze RM, Jawaid M, Nasir M, et al. Thermal stability of natural fibers and their polymer composites. Iran Polym J. 2020;29(7):625–48. doi:10.1007/s13726-020-00824-6.
62. Muralidhar BA. Viscoelastic and thermal behaviour of flax preforms reinforced epoxy composites. J Ind Text. 2015;44(4):542–52. doi:10.1177/1528083713502999.
63. Vahabi H, Ferry L, Longuet C, Sonnier R, Negrell-Guirao C, David G, et al. Theoretical and empirical approaches to understanding the effect of phosphonate groups on the thermal degradation for two chemically modified PMMA. Eur Polym J. 2012;48(3):604–12. doi:10.1016/j.eurpolymj.2011.12.015.
64. Laoutid F, Bonnaud L, Alexandre M, Lopez-Cuesta JM, Dubois P. New prospects in flame retardant polymer materials: from fundamentals to nanocomposites. Mater Sci Eng R Rep. 2009;63(3):100–25. doi:10.1016/j.mser.2008.09.002.
65. Wang H, Wang S, Du X, Wang H, Cheng X, Du Z. Synthesis of a novel flame retardant based on DOPO derivatives and its application in waterborne polyurethane. RSC Adv. 2019;9(13):7411–9. doi:10.1039/c8ra09838g.
66. Kung HC, Hsieh YK, Huang BW, Cheruiyot NK, Chang-Chien GP. An overview: organophosphate flame retardants in the atmosphere. Aerosol Air Qual Res. 2022;22(7):220148. doi:10.4209/aaqr.220148.
67. Schartel B. Phosphorus-based flame retardancy mechanisms—Old hat or a starting point for future development? Materials. 2010;3(10):4710–45. doi:10.3390/ma3104710.
68. Li S, Ren J, Yuan H, Yu T, Yuan W. Influence of ammonium polyphosphate on the flame retardancy and mechanical properties of ramie fiber-reinforced poly(lactic acid) biocomposites. Polym Int. 2010;59(2):242–8. doi:10.1002/pi.2715.